Active Generation and Propagation of Ca^{2+} Signals within Tunneling Membrane Nanotubes

Ian F. Smith,[†*] Jianwei Shuai,[§] and Ian Parker[†‡]
[†]Department of Neurobiology and Behavior and [‡]Department of Physiology and Biophysics, University of California, Irvine, California; and [§]Department of Physics, Xiamen University, Xiamen, China

ABSTRACT A new mechanism of cell-cell communication was recently proposed after the discovery of tunneling nanotubes (TNTs) between cells. TNTs are membrane protrusions with lengths of tens of microns and diameters of a few hundred nanometers that permit the exchange of membrane and cytoplasmic constituents between neighboring cells. TNTs have been reported to mediate intercellular Ca^{2+} signaling; however, our simulations indicate that passive diffusion of Ca^{2+} ions alone would be inadequate for efficient transmission between cells. Instead, we observed spontaneous and inositol trisphosphate (IP_3)-evoked Ca^{2+} signals within TNTs between cultured mammalian cells, which sometimes remained localized and in other instances propagated as saltatory waves to evoke Ca^{2+} signals in a connected cell. Consistent with this, immunostaining showed the presence of both endoplasmic reticulum and IP_3 receptors along the TNT. We propose that IP_3 receptors may actively propagate intercellular Ca^{2+} signals along TNTs via Ca^{2+}-induced Ca^{2+} release, acting as amplification sites to overcome the limitations of passive diffusion in a chemical analog of electrical transmission of action potentials.

Received for publication 15 December 2010 and in final form 10 March 2011.

*Correspondence: ismith@uci.edu

Cells have long been known to employ gap junctions and synapses to communicate with their neighbors. A recent study (1) described a new route of cell-cell communication via tunneling nanotubes (TNTs; membrane protrusions, a few hundred nanometers in diameter, that physically link cell bodies over distances of tens of micrometers). These membrane tubes have been observed in diverse cell types in vitro and in vivo, contain F-actin, and are characteristically distinct from other cellular protrusions in that they lack contact to the substratum. TNTs have been shown to transfer membrane-bound components such as lipids and proteins between cells, to permit transfer of organelles such as mitochondria, and to facilitate intercellular transfer of pathogens such as bacteria, HIV-1, and prion (2). TNTs have also been shown to mediate transmission of intercellular Ca^{2+} signals (3,4) in a manner that is analogous to the well-established intercellular transmission of Ca^{2+} waves via gap junctions but enables transmission between cells that are not in intimate contact.

To investigate whether passive diffusion of Ca^{2+} ions along TNTs might be sufficient to enable cell-cell communication, we simulated diffusion between two cells connected by TNTs of different radii and lengths containing 100 μM immobile cytosolic Ca^{2+} buffer (see Fig. S1 in the Supporting Material). At 10 s after a large (10 μM) step increase in cytosolic free [Ca^{2+}] in one cell, the Ca^{2+} flux (current) from the end of a 30 μm TNT with a typical diameter of 200 nm was <1 fA. Given that openings of a single inositol trisphosphate receptor (IP_3R) channel Ca^{2+} passing a current of ~100 fA (5) generally fail to trigger Ca^{2+}-induced Ca^{2+} release (CICR) (6), passive diffusion alone appears to be inadequate for robust intercellular transmission of Ca^{2+} signals via TNTs.

We therefore looked for evidence of active Ca^{2+} signaling within TNTs by employing cultured SH-SY5Y neuroblastoma and HEK cell lines in which we had previously characterized Ca^{2+} signaling mechanisms. TNTs were present in both cell types and displayed properties consistent with those previously reported (2). They were suspended in the medium above the base of the imaging dish (Fig. 1 *A*), contained F-actin but little or no tubulin (Fig. 1 *B*), attained lengths as great as 70 μm, and allowed interchange of mitochondria between cells, demonstrating cytosolic continuity between the TNT and cell body (Movie S1). Of note, in the context of Ca^{2+} signaling, the TNTs contained extensions of the endoplasmic reticulum (ER; Fig. 1 *C*) and expressed type 1 IP_3Rs along their length (Fig. 1 *D*). The IP_3R channel mediates liberation of Ca^{2+} ions sequestered in the ER, and its opening is promoted by IP_3 and cytosolic Ca^{2+}, leading to regenerative CICR (7) that may remain localized as Ca^{2+} puffs or propagate as a Ca^{2+} wave (8).

To investigate whether TNTs display localized Ca^{2+} signals independently of their connected cells, we incubated cells with membrane permeant-esters of the Ca^{2+} indicator Fluo-4, caged iIP_3, and the slow Ca^{2+} buffer EGTA (9). Fig. 2 *A* illustrates a TNT that was initially quiescent but generated recurring localized transient fluorescence Ca^{2+} signals after the iIP_3 was photoreleased by a UV flash that illuminated the entire imaging field. These localized fluorescence signals had a mean amplitude $\Delta F/F_0$ of 0.43 $\pm$ 0.05,

Editor: Leslie M. Loew.

doi: 10.1016/j.bpj.2011.03.007

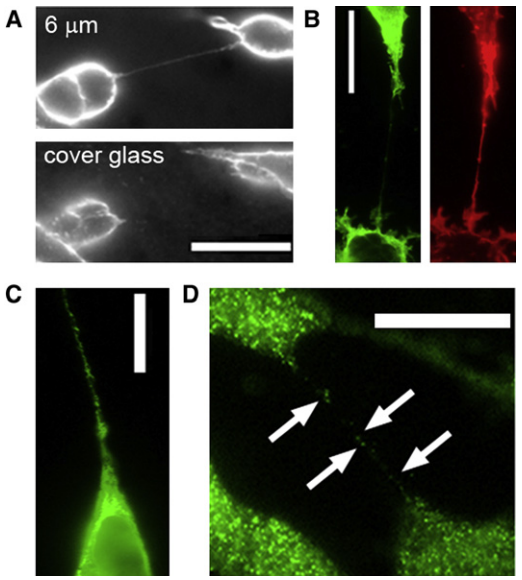

FIGURE 1 TNTs between cultured SH-SY5Y cells. (*A*) Cells stained with the fluorescent membrane dye Di-8-ANEPPQ showing a TNT suspended ~6 μm above the coverglass. Images were obtained focused at the coverglass (*bottom*) and 6 μm higher (*top*). (*B*) Immunofluorescence staining for tubulin (*green*) and F-actin (*red*, phalloidin 647). (*C*) SH-SY5Y cell transfected 24 h previously to express ER-GFP showing the presence of ER in a TNT. (*D*) Immunofluorescence staining of type 1 IP_3Rs along a TNT. All scale bars are 20 μm. Images are representative of $\geq$8 TNTs.

mean duration (at half-maximal amplitude) of 68 $\pm$ 25 ms, and spatial spread (full width at half-maximal amplitude) of 1.1 $\pm$ 0.11 μm ($n = 7$ sites). Except for being essentially constrained along one spatial dimension, local Ca^{2+} events in TNTs thus closely resemble the IP_3-mediated Ca^{2+} puffs that arise from discrete clusters of IP_3R within the bodies of many cell types (6,8). Moreover, local events in TNTs were spaced 4–6 μm apart (Fig. 2 *A*), in similarity to the distribution of puff sites in the cell body (6).

We also observed spontaneous Ca^{2+} events along TNTs ($n = 16$) even without photorelease of IP_3 and in cells that were not loaded with caged iIP_3. Fig. 2 *D* shows an instance in which Ca^{2+} signals initially remained localized but a localized event subsequently triggered a regenerative wave of Ca^{2+} that propagated in a saltatory manner across neighboring release sites with a velocity of ~8 $\mu m\ s^{-1}$. The localized signals persisted in the absence of external Ca^{2+} (medium with zero added Ca^{2+} and 1 mM EGTA), indicating that they involve a liberation of intracellular Ca^{2+} and not an influx of extracellular Ca^{2+}. Moreover, SH-SY5Y and HEK293 cells lack ryanodine receptors (RyRs; the other major class of ER Ca^{2+} release channels), and signals were inhibited by 20 mM caffeine, an IP_3R antagonist but RyR agonist (9/12 TNTs with spontaneous events in control: 3/14 after caffeine). Thus, the spontaneous events also appear to primarily involve IP_3Rs rather than RyRs, and may arise because of endogenous basal IP_3 within TNTs.

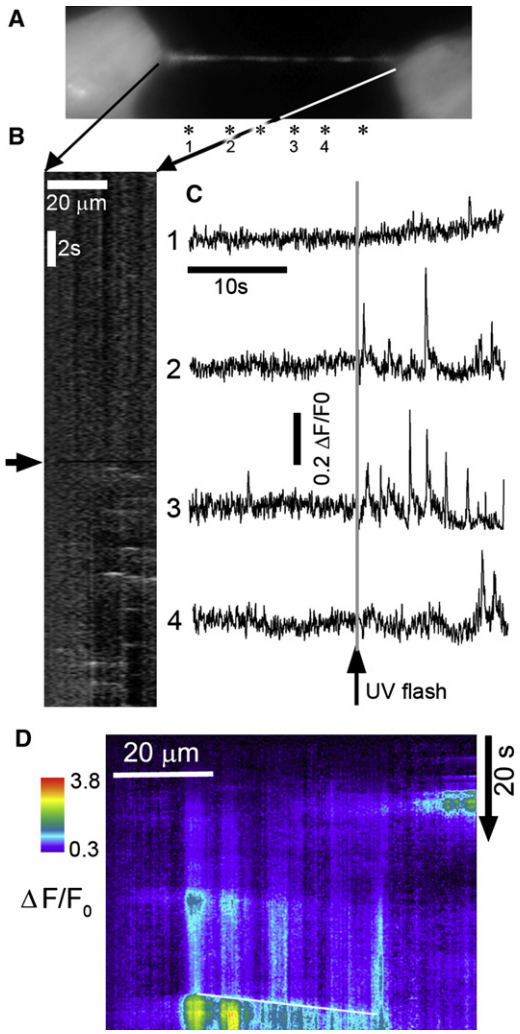

FIGURE 2 IP_3-evoked (*A–C*) and spontaneous (*D*) local Ca^{2+} events along TNTs. (*A*) Monochrome image shows resting fluo-4 fluorescence in a TNT bridging two HEK cells. Asterisks indicate locations of local Ca^{2+} events. (*B*) Linescan image derived by measuring Ca^{2+}-dependent fluorescence along the TNT (*abscissa*) as a function of time (*ordinate*). The arrow indicates when a photolysis flash was delivered. (*C*) Numbered traces show fluorescence signals measured from corresponding regions of the TNT marked in *A*. (*D*) Linescan image from a TNT bridging SH-SY5Y cells illustrating spontaneous local Ca^{2+} signals and their coordination to generate a propagating Ca^{2+} wave (marked by the *white diagonal line*).

The observation of active, local IP_3-mediated Ca^{2+} signals within TNTs suggests that they may facilitate Ca^{2+} wave propagation between cells. We investigated this possibility by focusing a small (~8 μm diameter) UV spot onto one cell of a pair bridged by a TNT to evoke Ca^{2+} liberation. This technique achieved a highly selective stimulation of the illuminated cell in that closely adjacent cells (not connected via TNTs) failed to respond, whereas in our hands an approach using local mechanical stimulation was confounded by intercellular Ca^{2+} waves mediated by extracellular release of ATP. As shown in Fig. 3, local uncaging of iIP_3 evoked

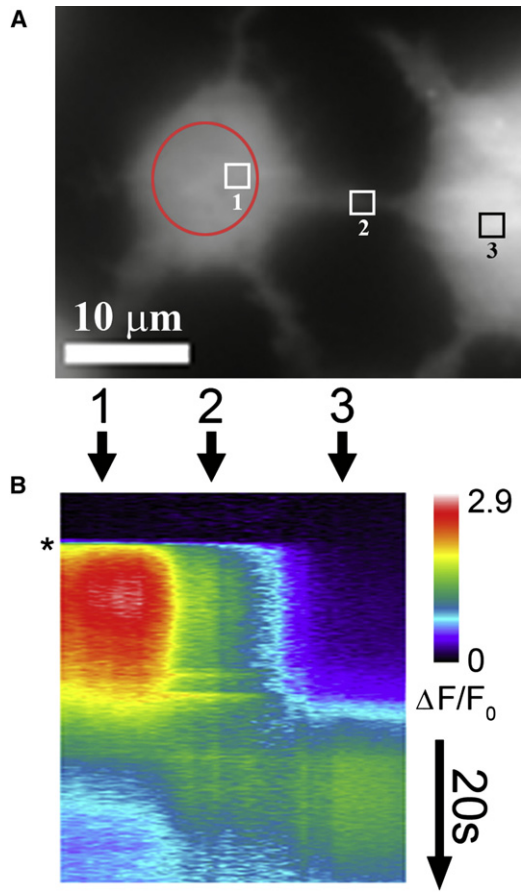

FIGURE 3 Active Ca^{2+} release in TNTs promotes intercellular transmission of Ca^{2+} signals. (*A*) Resting fluorescence image showing a TNT bridging adjacent SH-SY5Y cells. The red circle indicates the UV photolysis spot. Numbered regions correspond to regions in *B*. (*B*) Linescan image of Ca^{2+} signals in each cell and along the TNT. The asterisk indicates when a photolysis flash was delivered.

a strong Ca^{2+} signal in the leftmost cell; however, although this produced a rapid spread of Ca^{2+} down the TNT, the connected cell failed to respond for ~20 s. We then observed two successive, transient local responses within the TNT (region 2 in Fig. 3 *B*). These responses were associated with a clear increase in Ca^{2+} fluorescence in the second cell. This evoked a global regenerative response in that cell, which subsequently back-propagated into the TNT. Another example of robust cell-cell communication of global Ca^{2+} signals ($n = 8$) is illustrated in Movie S2. In other cases ($n = 17$; e.g., Movie S3), we observed small Ca^{2+} increases and local puffs in connected cells, although we also observed instances in which there was no detectable response ($n = 22$; e.g., Movie S4). Intercellular communication of Ca^{2+} signals persisted in Ca^{2+}-free medium ($n = 4$), ruling out the possibility that this was mediated via synaptic transmission.

In conclusion, our results demonstrate the presence of functional IP_3R Ca^{2+} release channels along the length of TNTs between cultured SH-SY5Y and HEK cells. Through successive cycles of Ca^{2+} release, diffusion, and CICR, these channels may serve as active amplification sites to promote propagation of Ca^{2+} signals along TNTs. Opening of IP_3R channels absolutely requires IP_3 as well as Ca^{2+} (7). Our simulations (Fig. S2) indicate that passive flux of IP_3 (which diffuses faster than Ca^{2+} (10)) from a stimulated cell could rapidly elevate $[IP_3]$ within a TNT so as to allow active wave propagation, but would only slowly raise $[IP_3]$ throughout the enormously larger volume of a connected cell. This may explain why connected cells often gave only small Ca^{2+} signals or failed to respond. Nevertheless, active transmission of Ca^{2+} waves along TNTs may be an efficient physiological mechanism for communication across a network of connected cells that are primed by a small basal elevation of cytosolic $[IP_3]$. We further speculate that other cell types may use an analogous mechanism mediated by RyRs that exhibit CICR without requiring a further second messenger.

SUPPORTING MATERIAL

Methods, model simulations, a reference, two figures, and four movies are available at http://www.biophysj.org/biophysj/supplemental/S0006-3495(11)00317-1.

ACKNOWLEDGMENTS

This work was supported by grants from the National Institutes of Health (GM 40871 to I.P., and GM65830 to I.P. and J.S.) and the National Natural Science Foundation of China (30970970), and the Specialized Research Fund for the Doctoral Program of Higher Education (20090121110028 to J.S.).

REFERENCES and FOOTNOTES

1. Rustom, A., R. Saffrich, …, H. H. Gerdes. 2004. Nanotubular highways for intercellular organelle transport. *Science.* 303:1007–1010.
2. Davis, D. M., and S. Sowinski. 2008. Membrane nanotubes: dynamic long-distance connections between animal cells. *Nat. Rev. Mol. Cell Biol.* 9:431–436.
3. Hase, K., S. Kimura, …, H. Ohno. 2009. M-Sec promotes membrane nanotube formation by interacting with Ral and the exocyst complex. *Nat. Cell Biol.* 11:1427–1432.
4. Watkins, S. C., and R. D. Salter. 2005. Functional connectivity between immune cells mediated by tunneling nanotubules. *Immunity.* 23:309–318.
5. Vais, H., J. K. Foskett, and D. O. Daniel Mak. 2010. Unitary calcium current through recombinant type 3 inositol triphosphate receptor channels under physiological ionic conditions. *J. Gen. Physiol.* 136:687–700.
6. Smith, I. F., S. M. Wiltgen, …, I. Parker. 2009. Ca^{2+} puffs originate from preestablished stable clusters of inositol trisphosphate receptors. *Sci. Signal.* 2:ra77.
7. Foskett, J. K., C. White, …, D. O. Mak. 2007. Inositol trisphosphate receptor Ca^{2+} release channels. *Physiol. Rev.* 87:593–658.
8. Yao, Y., J. Choi, and I. Parker. 1995. Quantal puffs of intracellular Ca^{2+} evoked by inositol trisphosphate in *Xenopus* oocytes. *J. Physiol.* 482:533–553.
9. Smith, I. F., S. M. Wiltgen, and I. Parker. 2009. Localization of puff sites adjacent to the plasma membrane: Functional and spatial characterization of calcium signaling in SH-SY5Y cells utilizing membrane-permeant caged IP3. *Cell Calcium.* 45:65–76.
10. Allbritton, N. L., T. Meyer, and L. Stryer. 1992. Range of messenger action of calcium ion and inositol 1,4,5-trisphosphate. *Science.* 258:1812–1815.

Supporting Material: Active generation and propagation of Ca^{2+} signals within tunneling membrane nanotubes

Ian F. Smith[1] Jianwei Shuai [3] & Ian Parker [1,2]

[1]Neurobiology and Behavior, [2] Physiology & Biophysics, University of California, Irvine, CA, 92697, USA. [3] Department of Physics, Xiamen University, Xiamen, China.

METHODS

CELL CULTURE: Human neuroblastoma SH-SY5Y cells were cultured in a mixture of Ham's F12 medium and Eagle's minimal essential medium (1:1 mixture), supplemented with 10% (v/v) fetal calf serum and 1% nonessential amino acids. Cells were incubated at 37 °C in a humidified incubator gassed with 95% air and 5% CO_2, passaged every 7 days and used for up to 20 passages. Cells were harvested in phosphate-buffered saline (PBS) without Ca^{2+} or Mg^{2+} and sub-cultured on glass coverslips at a seeding density of 3×10^4 cells/ml for 4 days before use. HEK cells were cultured in a similar manner except for use of DMEM supplemented with 10% (v/v) fetal calf serum as the culture medium. Prior to imaging, cells were incubated at room temperature in HEPES-buffered saline (HBS - composition in mM; NaCl 135, KCl 5, $MgCl_2$ 1.2, $CaCl_2$ 2.5, HEPES 5, and glucose 10) containing 1 μM ci-IP_3/PM for 45 mins, after which 1 μM fluo-4AM was added to the loading solution for a further 45 min before washing and allowing at least 30 mins for desterification. A further 60 min incubation with 5 μm EGTA-AM was performed for experiments studying localized Ca^{2+} signals within TNTs (Figs 2A,B & C), but was omitted for experiments on cell-cell communication of Ca^{2+} signals (Figs. 2D & 3 and Supplemmental Movies 2, 3 & 4)

CALCIUM IMAGING: Imaging of changes in $[Ca^{2+}]_i$ was accomplished using a home-built microscope system that was used in wide-field epifluorescence mode. The system was based around an Olympus IX 70 microscope equipped with an Olympus 60x oil objective (N.A. 1.45). Excitation light from a solid-state 488 nm laser (Coherent Sapphire) was reflected by a dichroic mirror and brought to a focus at the rear focal plane of the objective. An adjustable rectangular aperture placed at a conjugate image plane in the excitation path restricted illumination to the imaging field of the camera, and the aperture was overfilled by collimated laser light emerging from a 10x beam expander to provide Koehler illumination. Emitted fluorescence was collected through the same objective, passed through an Olympus fluorescence cube (490 nm dichroic, 510–600 nm bandpass barrier filter) and imaged using either a Cascade 128+ or Cascade 650 electron-multiplied c.c.d. camera (Roper Scientific). Photolysis of caged iIP_3 was accomplished by UV (350-400 nm) light from a shuttered mercury arc lamp, either delivered uniformly across the imaging field, or restricted to a single cell by a circular field-stop aperture.

IMMUNOFLUORESENCE MICROSCOPY: Cells were washed twice in PBS and fixed in 4% paraformaldehyde for 20 mins at room temperature. The fixed cells were then washed twice in PBS and permeabilized in PBS containing 0.05% Triton X100 and 10% normal goat serum (NGS) for 20 mins at room temperature. Permeabilized cells were then washed in PBS-NGS and incubated overnight with the appropriate antibody (Anti-IP_3R1, AB5882 at 1:1K, Anti-β-tubulin, T4026 at 1:1K and Alexa fluor 647 phalloidin at 1:1K). The next day, cells were washed three times with PBS and incubated (if needed) with fluorescently conjugated secondary antibodies at 1:1K. Cells were then washed three times prior to analysis.

To visualize TNTs by membrane staining, cells were incubated with the fluorescent lipophyllic dye Di-8-ANEPPQ (1 μM). The ER was visualized by transfecting cells with 1μg of a DNA construct encoding ER-GFP 24 hr prior to imaging. Mitochondria were visualized by transfection with a DNA construct for Mito-DsRed-Express.

MATERIALS: The membrane permeant caged IP_3 analogue ci-IP3/PM (D-2,3-O-Isopropylidene-6-O-(2-nitro-4,5-dimethoxy)benzyl-myo-Inositol 1,4,5-trisphosphate-Hexakis (propionoxymethyl) Ester) was diluted in pluronic F-127 (20% solution in DMSO) to a stock concentration of 200 μM and frozen down into 2 μl aliquots until needed. ci-IP_3/PM was purchased from SiChem (Bremen, Germany). EGTA-AM, Fluo-4 AM, Di-8-ANEPPQ, Alexa fluor 647 phalloidin ER tracker, pluronic F-127 were from Molecular Probes/Invitrogen (Carlsbad, CA). Anti-IP_3R1 antibody (AB5882) was purchased from Millipore, All other reagents including Anti-β-Tubulin (T4026) were purchased from Sigma (St. Louis). Mito-DsRed-Express was a kind gift from Joseph Dynes, UCI.

MODEL SIMULATIONS

NANOTUBE MODEL: We modelled a nanotube connecting two cells as a cylindrical tube with a radius of *r* and a length of *L*. The following species were present

within the cell cytoplasm and the nanotube: free Ca^{2+} ions ($[Ca^{2+}]$), stationary Ca^{2+} buffer in free and Ca^{2+}-bound ([SCa]) forms, mobile Ca^{2+} buffer in free and Ca^{2+}-bound ([MCa]) forms, and free IP_3. The simple Euler difference method was used to solve the partial differential equations with a time increment $\Delta t = 2$ μs and spatial grid distance $\Delta x = 50$ nm

Ca^{2+} DIFFUSION ALONG THE NANOTUBE: The following parameter values were assumed: Diffusion coefficients for free Ca^{2+}, mobile buffer and IP_3 messenger were $D_{\mathrm{Ca}} = 200$ μm^2/s, $D_{\mathrm{MCa}} = 50$ μm^2/s, $D_{\mathrm{IP3}} = 280$ μm^2/s, respectively; total concentration of stationary Ca^{2+} buffer $S_T = 100$ μM with calcium binding and unbinding rates $\alpha_S = 50$ μM^{-1}s^{-1} and $\beta_S = 100$ s^{-1}; the indicator dye buffer was considered the sole mobile Ca^{2+} buffer with total concentration $M_T = 20$ μM and calcium binding and unbinding rates $\alpha_M = 150$ μM^{-1}s^{-1} and $\beta_M = 450$ s^{-1}.

The diffusion equation for free Ca^{2+} ions ($[Ca^{2+}]$) in the nanotube with diffusion coefficient D_{Ca} is described as follows:

$$\frac{\partial[\mathrm{Ca}^{2+}]}{\partial t} = D_{\mathrm{Ca}}\nabla^2[\mathrm{Ca}^{2+}] + \beta_{\mathrm{S}}\times[\mathrm{SCa}] - \alpha_{\mathrm{S}}\times[\mathrm{Ca}^{2+}]\cdot(S_{\mathrm{T}} - [\mathrm{SCa}]) + \beta_{\mathrm{M}}\times[\mathrm{MCa}] - \alpha_{\mathrm{M}}\times[\mathrm{Ca}^{2+}]\cdot(M_{\mathrm{T}} - [\mathrm{MCa}])$$

in which ∇^2 is the Laplace operator.

For Ca^{2+}-bound stationary buffer ([SCa]),

$$\frac{\partial[\mathrm{SCa}]}{\partial t} = \alpha_{\mathrm{S}}\times[\mathrm{Ca}^{2+}]\times(S_{\mathrm{T}} - [\mathrm{SCa}]) - \beta_{\mathrm{S}}\times[\mathrm{SCa}]$$

For Ca^{2+}-bound mobile buffer ([MCa]) with diffusion coefficient D_{MCa},

$$\frac{\partial[\mathrm{MCa}]}{\partial t} = D_{\mathrm{MCa}}\nabla^2[\mathrm{MCa}] + \alpha_{\mathrm{M}}\times[\mathrm{Ca}^{2+}]\times(M_{\mathrm{T}} - [\mathrm{MCa}]) - \beta_{\mathrm{M}}\times[\mathrm{MCa}]$$

Because of the radial symmetry in the TNT, Ca^{2+} diffusion is described in one dimension along its length.

The resting concentrations of Ca^{2+}-bound stationary buffer and Ca^{2+}-bound mobile buffer are given by;

$$S_{\mathrm{T}}/(1+\beta_{\mathrm{S}}/(\alpha_S\times[\mathrm{Ca}^{2+}]_{\mathrm{Rest}}))$$

and $M_{\mathrm{T}}/(1+\beta_{\mathrm{M}}/(\alpha_{\mathrm{M}}\times[\mathrm{Ca}^{2+}]_{\mathrm{Rest}}))$, respectively.

We consider a case in which the Ca^{2+} concentration in the first cell is stepped from 50 nM to 10 μM, simulating a large and sustained Ca^{2+} liberation in that cell. $[Ca^{2+}]$ in the second cell then increases with time due to the Ca^{2+} diffusion through the TNT. In light of the small amounts of Ca^{2+} that pass through the TNT, we make a simplifying assumption that Ca^{2+} concentrations in each cell are homogeneous throughout the cytosol.The equation for free Ca^{2+} concentration in the second cell is then described by;

$$d[\mathrm{Ca}^{2+}]/dt = J_{\mathrm{Ca}}/V + \beta_{\mathrm{S}}\times[\mathrm{SCa}] - \alpha_{\mathrm{S}}\times[\mathrm{Ca}^{2+}]\cdot(S_{\mathrm{T}} - [\mathrm{SCa}]) + \beta_{\mathrm{M}}\times[\mathrm{MCa}] - \alpha_{\mathrm{M}}\times[\mathrm{Ca}^{2+}]\cdot(M_{\mathrm{T}} - [\mathrm{MCa}])$$

with V the cell volume and J_{Ca} the flux of free calcium from the TNT to the second cell which is given by;

$$J_{\mathrm{Ca}} = D_{\mathrm{Ca}}\times S\times\partial[\mathrm{Ca}^{2+}]/\partial x\big|_{\mathrm{TNT\ Boundary}}.$$

with S the lateral area of TNT. Similar equations apply for Ca^{2+}-bound mobile buffer with a flux and for Ca^{2+}-bound stationary buffer .

In Fig. S1 we show the resulting Ca^{2+} flux (expressed as Ca^{2+} current) passing from TNTs of various radii and lengths into the second cell at a time 10s after $[Ca^{2+}]$ in the first cell is stepped to 10 μM. For a 'typical' TNT with a length of 30 μm and a diameter of 200 nm the Ca^{2+} current after 10s is less than 1 fA; or less than 1% of the Ca^{2+} current through a single IP_3R channel. Fig. S1 further shows that the predicted Ca^{2+} current from the TNT falls precipitously for TNT lengths over 50 μm. This arises because Ca^{2+} diffusion along the TNT is hindered by binding to immobile buffers. In effect, a front of Ca^{2+} advances slowly along the TNT as the buffer comes into equilibrium behind it, and a negligible amount of Ca^{2+} will exit from the TNT until the front has progressed to the end. Thus, passive propagation of Ca^{2+} signals along TNTs would be even less effective than indicated by the above example for longer distances, and at shorter times for shorter TNTs.

IP_3 DIFFUSION ALONG THE NANOTUBE: We also consider the diffusion of IP_3 along a nanotube from a stimulated cell to a connected, unstimulated cell, described as follows:

$$\frac{\partial[\mathrm{IP}_3]}{\partial t} = D_{\mathrm{IP3}}\nabla^2[\mathrm{IP}_3]$$

In Fig. S2 we show how IP_3 diffusion would change $[IP_3]$ within a TNT and within a connected cell following a step increase of $[IP_3]$ in the first cell. We consider two cells each with a radius of 5 μm, and assume for simplicity that $[IP_3]$ is homogeneous throughout the cytosol of both cells. The cells are connected by a TNT of 50 μm length and we consider radii of 50, 100 and 200 nm, as indicated. The concentration of IP_3 in both cells is initially zero, and is then stepped to a normalized value of 1 in one cell to simulate local photorelease of IP_3. The flux of IP_3 through the TNT changes $[IP_3]$ in both cells, as well as in the TNT, as shown in Fig. S2 as functions of time.

The concentration of IP_3 at a distance 30 μm along the TNT equilibrates within ~2s to a value about 40% of the initial value in the stimulated cell, suggesting that $[IP_3]$ would be sufficiently elevated to sustain CICR for an appreciable distance along the TNT. On the other hand, for a 100 nm radius TNT the concentration of IP_3 in the second cell increased to only about 5% of that in the stimulated cell even after 20 s.

The iIP_3 photoreleased in our experiments is metabolized more slowly than native IP_3, and we did not include a term for IP_3 degredation in our model. However, it is likely that metabolism of native IP_3 would not appreciably affect the ability of TNTs to propagate IP_3-dependent Ca^{2+} signals, because the degredation rate of ~60 s measured in oocytes (1) is slow in comparison to the timescale ($\leq$ 10s) for Ca^{2+} signal propagation via TNTs.

1. Sims, C.E. and N.L. Allbritton. 1998. Metabolism of inositol 1,4,5-trisphosphate and inositol 1,3,4,5-tetrakisphosphate by the oocytes of *Xenopus laevis*. J Biol Chem 273:4052-4058.

Supplementary Figures

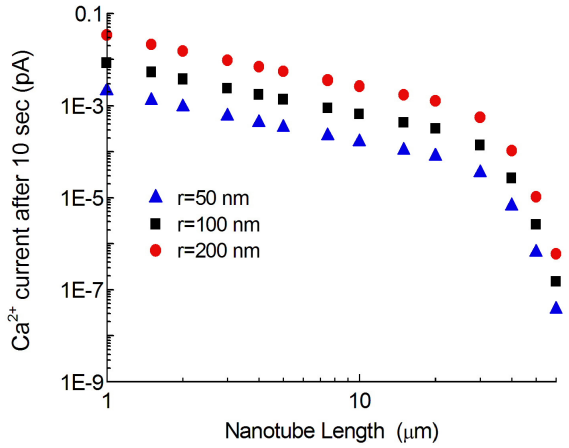

Figure S1: Passive flux of Ca^{2+} along a TNT from a stimulated cell into a connected cell. The plot shows simulations of two cells connected by a nanotube of varying length (indicated on the ordinate), and with radii of 50, 100 and 200 nm as indicated by different symbols. The Ca^{2+} concentration in both cells was initially 50 nM, and the concentration in one cell was then stepped to 10 μM. The data points show the resulting flux of Ca^{2+} from the end of the TNT into the second cell after 10s. Flux is expressed on the abscissa in terms of Ca^{2+} current: a current of 1pA is equivalent to about 5 x 10^{-18} moles s^{-1} of Ca^{2+}. Numerical methods and parameter values were as described in Supporting Methods.

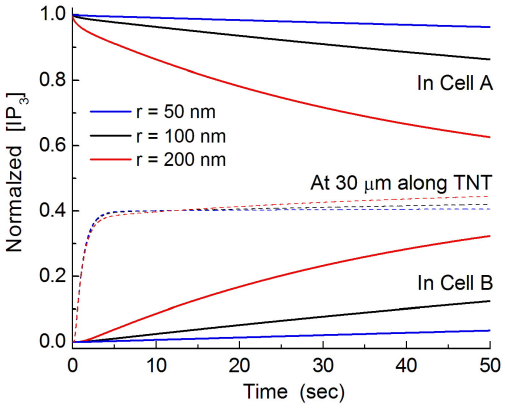

Figure S2: Passive diffusion of IP_3 along a TNT. The plot shows simulations of two cells (A and B), each with a radius of 5 μm connected by a nanotube 50 μm long and with radii of 50, 100 and 200 nm as indicated by different colors. The concentration of IP_3 in both cells was initially zero, and was then stepped to a normalized value of 1 in Cell A to simulate local photorelease of IP_3. The curves show the resulting changes in [IP_3] as functions of time after the step in cell A, in cell B, and at a distance of 30 μm along the TNT from cell A.

Supplementary Movies

Movie S1: Movement of mitochondria along TNTs into the cytosol of a neighboring SH-SY5Y cell. SH-SY5Y cells were transfected with 1 µg Mito-DsRed-Express and imaged 24 hr later. Time stamp reads in minutes:seconds.

Movie S2: Cell-cell communication of Ca^{2+} signals along TNTs. Panels show 'raw' fluorescence of fluo-4 (left), and Ca^{2+} signals ($\Delta F/F_0$; right) on a pseudocolor scale, with increasing [Ca^{2+}] corresponding to warmer colors. One cell was simulated after 4 s by local photorelease of iIP_3 from a UV light spot focused as indicated by the circle in the first frame. The evoked rise in Ca^{2+} was then transmitted along a TNT to induce a rise in Ca^{2+} in a neighboring cell (below), which then further propagated to a third cell (upper left). Time stamp reads in minutes:seconds.

Movie S3: Example of cell-cell communication along a TNTs that evoked puffs, but not a global Ca^{2+} response in connected cells. Movie shows pseudocolored Ca^{2+} signals ($\Delta F/F_0$; right pane) evoked following local photorelease of iIP_3 by a UV light spot focused as indicated by the circle in the first frame. Puff activity was then stimulated in two adjacent cells connected via TNTs, and within the TNTs themselves. Time stamp reads in minutes:seconds.

Movie S4: Active propagation of Ca^{2+} signals along a TNT which failed to evoke a response in the connected cell. Panels show 'raw' fluorescence of fluo-4 (left), and Ca^{2+} signals ($\Delta F/F_0$; right) on a pseudocolor scale, with increasing [Ca^{2+}] corresponding to warmer colors. The uppermost cell was stimulated by a UV light spot focused on the soma to evoke a strong Ca^{2+} signal. Discrete localized Ca^{2+} events transmitted the rise in Ca^{2+} along the TNT, but failed to induce an appreciable rise in Ca^{2+} in the connected cell. This lack of communication was not due to the TNT being closed-ended as subsequent stimulation of the lower cell induced a passive flux of Ca^{2+} that diffused several microns into the TNT (not shown). Time stamp reads in minutes:seconds.